

## Pore-Size-Dependent Orientational Dynamics of a Liquid Crystal Confined in a Porous Glass

G. Schwalb and F. W. Deeg

*Institut für Physikalische Chemie, Universität München, 80333 München, Germany*

(Received 28 September 1994)

Time-resolved transient grating optical Kerr effect experiments were used to investigate the collective reorientational dynamics of pentylcyanobiphenyl embedded in the nanometer-length-scale pores of silica glasses. Measurements in the bulk pretransitional temperature range show a drastic decrease of the relaxation time of the order-parameter fluctuations compared to the bulk with a pronounced pore-size dependence. A Landau model based on independent pore segments can explain the pore-size dependence, but cannot satisfactorily reproduce the observed nonexponentiality of the decays.

PACS numbers: 64.70.Md, 68.45.Kg, 78.47.+p

In the past decade the study of finite size effects and surface interaction on the ordering, phase transitions, and structural properties of liquid crystals (LC) has attracted growing interest, both theoretically and experimentally. Previous work has concentrated on static properties in well-characterized confining geometries as planar [1], cylindrical [2], and spherical [3,4] cavities with length scales above 20 nm. These investigations have determined the nematic director configuration of these systems, the existence of ordered surface layers inducing paranematic order in the isotropic phase, and shifts of the phase transition temperature. In the case of a spherical droplet of 20 nm diameter, even continuous ordering instead of the usual weakly first order transition was observed [4].

Recently, studies have been extended to randomly confining systems like the three-dimensional connected pore network of Vycor glass and silica aerogel. In these porous systems it is possible to achieve spatial restrictions well below 20 nm, the typical magnitude of the order-parameter correlation length at the isotropic to nematic phase transition. Because of this severe confinement and the randomness of the structure, new static and dynamical effects appear [5–8]. The theory of critical phenomena also suggests interesting comparisons of data for LC/porous-glass systems with corresponding results for binary mixtures [9] and  $^4\text{He}$  [10] inside these porous systems.

Light scattering and calorimetric measurements *below* the bulk nematic-isotropic phase transition temperature  $T_{NI}(\text{bulk})$  of octylcyanobiphenyl (8CB) in a silica aerogel with a mean pore size of 175 Å showed a continuous ordering with an orientational correlation length not exceeding the pore size, suggesting a multidomain nematic structure [5]. Similar results were obtained from a nuclear magnetic resonance and calorimetric study of pentylcyanobiphenyl (5CB) in Vycor glass with 70 Å mean diameter [6]. These data are compatible with a small but nonzero mean order parameter  $Q$  inside essential independent pore segments, increasing continuously with decreasing temperature, with no evidence of a nematic-isotropic

phase transition. Using a simple Landau model a mean value of  $Q \sim 0.025$  at  $T_{NI}(\text{bulk})$  can be estimated.

On the other hand, studies of the dynamical properties of confined nematogens are scarce. A dynamic light scattering experiment on 8CB in aerogel with a mean pore size of 200 Å has discovered deviations from the bulk dynamical behavior *below*  $T_{NI}(\text{bulk})$  [8]. Compared to the bulk a much slower relaxation time for the fluctuations of the orientational order parameter was found. The logarithmic scaling observed for the order-parameter autocorrelation function was explained by a random field Ising type approach, based on the argument that the percolating structure of the glass imposes a random uniaxial field on the liquid crystal. Although the first attempts to translate the conventional random field theory to LC/porous systems can account for the absence of hysteresis [11], the functional form of the autocorrelation function cannot be explained so far. In the temperature range *above*  $T_{NI}(\text{bulk})$  and within the limited time resolution of the used apparatus, the confined system showed a fast decay in the  $10^{-7}$  s range, undistinguishable from bulk 8CB. This fast component also made a small contribution to the relaxation dynamics *below*  $T_{NI}(\text{bulk})$ . It is this *fast* decay in the bulk pretransitional regime that we have investigated in a study of 5CB confined in silica porous glasses. For the first time different pore sizes and modified pore surfaces were studied allowing us to explicitly determine the influence of finite size and surface interaction on the order-parameter relaxation for a wide temperature range up to 80 K above the bulk phase transition.

5CB, purchased from Merck, has a well-defined weakly first order nematic-isotropic phase transition at  $T_{NI}(\text{bulk}) = 35.2^\circ\text{C}$ . The pseudonematic fluctuations in the isotropic phase are characterized by the correlation length  $\xi$  and the relaxation time  $\tau$ , both diverging on approaching the phase transition according to the Landau-de Gennes theory [12] as  $\xi = [L/a(T - T^*)]^{1/2}$  and  $\tau = \nu/a(T - T^*)$  with the isotropic elastic coefficient  $L \approx 17 \times 10^{-12}$  J/m,  $a = 0.132 \times 10^6$  J/m<sup>3</sup> K, with  $T^* = T_{NI} - 1.1^\circ\text{C}$  the supercooling limit and  $\nu$  a weakly

temperature dependent viscosity coefficient [2,13]. At  $T_{NI}(\text{bulk})$   $\xi$  and  $\tau$  have finite values of  $\xi \sim 200 \text{ \AA}$  and  $\tau$  on the order of several hundred nanoseconds.

The porous silica glasses, purchased from Geltech Inc., were characterized by  $N_2$  Brunauer-Emmett-Teller (BET) adsorption and desorption isotherms showing a well-defined narrow pore size distribution with mean pore diameters of 100, 50, and 25  $\text{\AA}$ , half widths at half maximum of 48, 23, and 13  $\text{\AA}$ , specific surface areas of 432, 619, and 666  $\text{m}^2/\text{g}$ , and porosities of 65%, 61%, and 47%, respectively. The surface of the pores is covered with polar OH groups. Chemical treatment with dichlorodimethylsilane allows one to replace these polar OH groups with less polar groups of  $-\text{OSi}(\text{CH}_3)_2\text{OC}_2\text{H}_5$  and systematically alter the surface interaction with the polar 5CB molecules. In order to distinguish surface effects and finite size effects, a surface-modified sample with mean pore diameter of 100  $\text{\AA}$  (100  $\text{\AA}$  M) was also used in this investigation. The disk-shaped samples (10 mm diameter, 5 mm thickness) were immersed in a spectroscopic cuvette filled with isotropic 5CB and left several days to ensure complete filling. The cuvette was inserted into a variable temperature cell whose temperature could be controlled within  $\pm 0.1 \text{ K}$ .

The orientational relaxation dynamics of the order-parameter fluctuations are directly probed with a transient grating (TG) optical Kerr effect setup [13]. Two coherent time-coincident excitation pulses with perpendicular polarization overlap in the sample to form an optical interference pattern and create a spatially modulated orientational anisotropy via the optical Kerr effect. The decay of this anisotropy is probed by a variably time-delayed probe pulse which is Bragg scattered off this grating. Neglecting absorption, the scattered intensity  $I(t) \propto |\chi^{(3)}(t)|^2 \propto |\delta\epsilon(t)|^2 \propto |G(t)|^2$ , where  $\chi^{(3)}$  is the third-order nonlinear susceptibility,  $\delta\epsilon$  the induced peak-null difference of the dielectric constant in the optical grating, and  $G(t)$  the dielectric response function of the system. As an optical grating is generated solely in the overlap region of the excitation beams, spatial translations of the cuvette allow one to probe either the confined or the bulk liquid. As a drawback this cell design limits the experiments to the bulk isotropic temperature range because of the strong nematic scattering. A more detailed description of the laser apparatus and experimental setup can be found elsewhere [14].

TG signals of bulk 5CB and 5CB in the different porous glass samples at the temperature of  $42^\circ\text{C}$  are shown in Fig. 1. With the experimental time resolution of 100 ps the bulk reorientational dynamics are characterized by an instantaneous response at  $t = 0$  with a fast decay within less than 1 ns, representing noncollective molecular reorientation, which is essential temperature independent up to  $70^\circ\text{C}$  [13]. The following monoexponential decay on the ns time scale is characteristic of the relaxation dynamics of the order-parameter fluctuations in the isotropic phase,

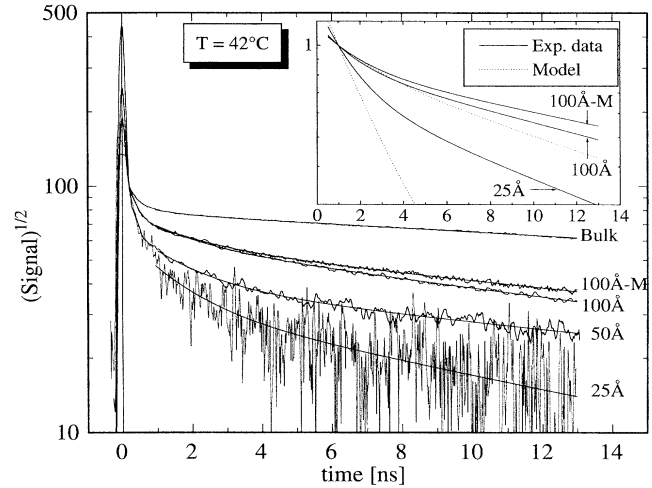


FIG. 1. TG signal and biexponential fit at  $T = 42^\circ\text{C}$  for bulk 5CB and for 5CB confined to porous-glass samples with mean diameters of 100, 50, and 25  $\text{\AA}$  (all untreated) as well as the surface-modified 100  $\text{\AA}$  sample (100  $\text{\AA}$  M). For better comparison an oscillatory contribution in the porous sample data has been subtracted (see text). The inset compares the experimental with the simulated decays at  $42^\circ\text{C}$  for the 100 and 25  $\text{\AA}$  pore size.

showing the critical slowing down on approaching the phase transition mentioned above. It is evident that this slow collective orientational dynamics is also observed in the confined systems down to 25  $\text{\AA}$  pore-size sample. For better comparison with the bulk data, an oscillatory contribution in the porous sample data, originating from the optical generation of shear waves in the silica glasses by impulsive stimulated Brillouin scattering [15], has been subtracted. Clearly, the decay in the porous samples is faster than in the bulk, deviates from a monoexponential, and exhibits a strong pore size dependence. The decline of the signal-to-noise ratio is due to the decrease of absolute signal with decreasing pore size.

In the time window between 1 and 13 ns a biexponential fit of the nonexponential decay results in smaller residues and more robust results than a fit with, e.g., a stretched exponential. Because there is no obvious relationship to two different physical processes, a model independent approach to characterize the decay is used. Based on the biexponential fit of the data a mean relaxation rate  $\langle k \rangle = [t_2 - t_1]^{-1} \int_{t_1}^{t_2} k dt$  is evaluated with  $k = -R'(t)/R(t)$ ,  $R(t)$  the obtained biexponential fit function for each dataset, and  $t_1 \leq t \leq t_2$  the regarded time window of the decay.

An overview on the temperature and pore-size dependence of the resulting mean relaxation time  $\langle \tau \rangle = 1/\langle k \rangle$  together with the values in the bulk is depicted in Fig. 2. Two temperature ranges with very different behavior can be distinguished. A detailed analysis of the higher temperature range, where the reorientational dynamics of the

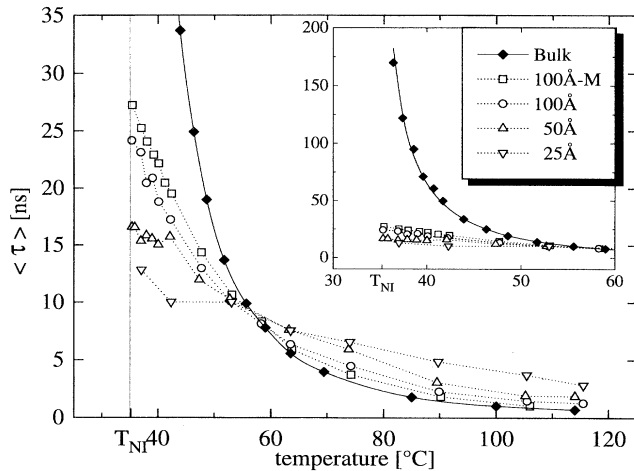


FIG. 2. Temperature dependence of the mean relaxation time as defined in the text, for bulk and confined 5CB samples. Data points for each sample are connected with dotted lines.

confined liquid is obviously slowed down compared to the bulk, was presented in a previous paper [16]. The comparison of the bulk, the surface-modified, and the untreated porous sample has revealed a slower component in addition to the bulk decay, which originates from a surface layer of 5CB molecules and which is barely observable in the surface-modified sample. In the low temperature range between 35 and 55 °C the mean relaxation time for the confined nematogen is strongly reduced and does not diverge for  $T \rightarrow T_{NI}(\text{bulk})$ , as can be seen in the inset of Fig. 2. Comparison between modified and unmodified samples lets us conclude that this result is dictated by the geometrical restriction of the pores and only insignificantly influenced by surface interactions. First, untreated and surface-modified sample exhibit qualitatively the same dynamics as evident in Fig. 1. Considering the pore-size dependence depicted in Figs. 1 and 2, the untreated 100 Å sample behaves like a surface-modified 100 Å sample with a smaller effective pore size. Second, around  $T = 60^\circ\text{C}$  a crossing of the relaxation times of the two samples occurs. This is due to the increasing contribution of a slower surface layer component in the experimental time window at high temperature for the case of the unmodified sample. These observations imply for the untreated sample a surface layer of LC molecules which contribute weakly or not at all to the orientational dynamics in the investigated time window and temperature range. This layer effectively reduces the pore size for the untreated samples.

In order to elucidate the observed reduction in relaxation time and the deviations from a monoexponential decay, the Landau ansatz of independent pore segments introduced by Iannacchione *et al.* was employed [6], using an effective scalar order parameter  $Q$  obtained by averaging over a pore. Accordingly the free energy

expansion for an independent pore segment yields

$$f = f_0 + \frac{1}{2} a(T - T^*)Q^2 - \frac{1}{3} bQ^3 + \frac{1}{4} cQ^4 + \frac{1}{2} \frac{L}{R^2} Q^2 - gQ, \quad (1)$$

where  $f_0$ ,  $a$ ,  $T^*$ ,  $b$ ,  $c$ , and  $L$  are temperature independent material parameter (for  $a$ ,  $T^*$ , and  $L$  see above) and  $R$  is the effective radius of pore curvature. The first four terms describe the bulk behavior. The distortion energy of the paranematic director field through the pore curvature is approximated by the term  $LQ^2/2R^2$ , whereas the pore-size independent  $gQ$  term describes the ordering effect due to interaction with the surface.

The dynamical consequences of this ansatz can be derived within the framework of a time-dependent Landau-Ginzburg description. Neglecting the influence of the shear rate tensor, the time variation of the order parameter is given by  $\nu \dot{Q} = -\partial f / \partial Q$  with  $\nu$  the viscosity coefficient mentioned above [12,17]. Following Mauger and Mills [17], one can write  $Q(t) = \bar{Q} + \delta Q(t)$  and separate this differential equation in a time-dependent and time-independent part. The time-dependent equation, which describes the fluctuations of  $Q$ , can be linearized with respect to  $\delta Q$ . Because the paranematic order is small in the temperature range above the bulk phase transition [6], the mixed terms  $b\bar{Q}\delta Q$  and  $c\bar{Q}^2\delta Q$  can be neglected yielding

$$\nu \delta \dot{Q} + [a(T - T^*) + L/R^2]\delta Q = \delta \mathcal{F}, \quad (2)$$

with  $\delta \mathcal{F}$  a fluctuating force, whose precise form is not required. The solution of this differential equation yields a *monoexponential* relaxation of  $\delta Q$  with  $\tau_R = \nu / a(T - T_R^*)$  introducing a pore size dependent  $T_R^* = T^* - L/aR^2$ . This renormalization of  $T^*$  by including the elastic energy in Eq. (1) was also found in the derivation of the static properties [6]. It should be stressed that in this simplified approach the surface interaction  $g$  has no influence on the relaxation time  $\tau_R$ .

The found pore-size dependence of  $\tau_R$  can, in fact, qualitatively explain our experimental results. Because of the strong pore-size dependence with  $\tau \sim R^2$ , for radii smaller than 200 Å and temperatures above  $T_{NI}(\text{bulk})$ , the finite distribution of pore curvatures inside the porous glass induces a distribution of relaxation rates leading to a nonexponential decay of the TG signal.

In order to verify if the model can account for the magnitude of the observed effect (see inset of Fig. 2), a simulation of the signal decay was carried out. The distribution of radii  $f(R)$  was taken from the  $N_2$  BET adsorption and desorption data of the porous glasses, neglecting a possible reduction of  $R$  by the surface layer. The theoretical signal decay was then obtained by the appropriate summation over the contributions from all pore sizes  $I(t) = \sum_{R_i} [f(R_i)/\tau_i] \exp(-t/\tau_i)$  with  $\tau(R_i)$

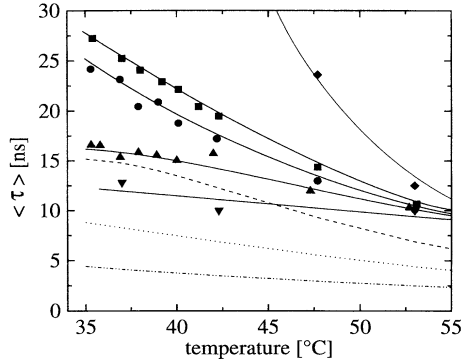


FIG. 3. Comparison of the mean relaxation time for the simulated (100 Å: ---, 50 Å: ·····, 25 Å: -·-·-·) and experimental data (bulk: ◆, 100 Å M: ■, 100 Å: ●, 50 Å: ▲, 25 Å: ▼). Solid lines provide a guideline to the eye.

as predicted by the Landau ansatz. For a comparison of the simulation with the experimental data the mean relaxation time  $\langle \tau \rangle$  was determined. Figure 3 shows the resulting temperature dependence of  $\langle \tau \rangle$  for three pore sizes in the temperature range 35 to 55 °C. The model reproduces roughly the experimentally observed magnitude of  $\tau$  as well as its temperature and pore-size dependence. But in general the simulated  $\langle \tau \rangle$ 's are too small with the deviations being more pronounced for smaller pore sizes. However, a detailed comparison of the simulated and experimental signal decays reveals that the nonexponentiality in the simulated data is less pronounced than in the experimental data (see inset of Fig. 1). To further characterize the nonexponentiality of the decay, the second momentum of  $\tau$  was used to calculate a width of the relaxation time distribution  $\Delta \tau = (\langle \tau^2 \rangle - \langle \tau \rangle^2)^{1/2}$ . To allow for a numerical comparison between the experimental and simulated data the resulting values are given in Table I for  $T = 42$  °C. Introduction of a fitting factor in the elastic term of the Landau expansion does not alleviate this discrepancy of the decay functions. To achieve the desired nonexponentiality of the decay, a much broader distribution of the pore radii would be necessary. In our opinion this suggests that it is necessary to include interporous interaction in the model to satisfactorily describe the dynamics. However, we cannot rule out that there are intrinsic deviations from an exponential relaxation, as, e.g., predicted by random field models.

TABLE I.  $\langle \tau \rangle \pm \Delta \tau$  as defined in the text for the experimental (E) and simulated (S) decays at  $T = 42$  °C.

	100 Å M	100 Å	50 Å	25 Å
E	$19.5 \pm 6.1$	$17.2 \pm 5.2$	$15.7 \pm 6.8$	$10.0 \pm 3.7$
S	$12.3 \pm 3.1$	$12.3 \pm 3.1$	$6.9 \pm 1.8$	$3.5 \pm 1.0$

In summary, we have presented the first investigation of the pore-size dependence of orientational dynamics in the nematic-isotropic transition region of a LC. The drastic reduction of the relaxation time with respect to the bulk can be qualitatively understood within a Landau ansatz assuming independent pore segments and taking into account the large elastic distortion energy introduced by the pore curvature. Considering the light scattering data from Bellini *et al.* [5], this result is consistent with a conventional scaling of correlation time and length. However, quantitative deviations between theory and experimental data, in particular a pronounced nonexponentiality of the decay, cannot be neglected. To focus on this problem, investigations of confined 5CB in the temperature range *below* the bulk phase transition temperature are under way. We are very curious how the transition from fast dynamics as observed in the experiments described here to the extremely slow dynamics as found in the study of Wu *et al.* [8] takes place.

We would like to thank C. Bräuchle for generous support of this work.

- [1] P. Sheng, Phys. Rev. Lett. **37**, 1059 (1976); Phys. Rev. A **26**, 1610 (1982); H. Yokoyama, J. Chem. Soc. Faraday Trans. 2 **84**, 1023 (1988).
- [2] G.P. Crawford, R. Stannarius, and J.W. Doane, Phys. Rev. A **44**, 2558 (1991); G.P. Crawford *et al.*, Phys. Rev. Lett. **66**, 723 (1991); G.P. Crawford *et al.*, Phys. Rev. Lett. **70**, 1838 (1993).
- [3] S. Kralj, S. Žumer, and D.W. Allender, Phys. Rev. A **43**, 2943 (1991); I. Vilfan, M. Vilfan, and S. Žumer, Phys. Rev. A **40**, 4724 (1989).
- [4] A. Golemme *et al.*, Phys. Rev. Lett. **61**, 2937 (1988).
- [5] T. Bellini *et al.*, Phys. Rev. Lett. **69**, 788 (1992).
- [6] G.S. Iannacchione *et al.*, Phys. Rev. Lett. **71**, 2595 (1993).
- [7] S. Tripathi, C. Rosenblatt, and F.M. Aliev, Phys. Rev. Lett. **72**, 2725 (1994).
- [8] X-L. Wu *et al.*, Phys. Rev. Lett. **69**, 470 (1992).
- [9] S.B. Dierker and P. Wiltzius, Phys. Rev. Lett. **66**, 1185 (1991); B.J. Frisken and D.S. Cannell, Phys. Rev. Lett. **69**, 632 (1992).
- [10] D. Finotello *et al.*, Phys. Rev. Lett. **61**, 1954 (1988); A. Wong and M.H. Chan, Phys. Rev. Lett. **65**, 2567 (1990).
- [11] A. Maritan *et al.*, Phys. Rev. Lett. **67**, 1821 (1991); Phys. Rev. Lett. **72**, 4113 (1994).
- [12] F.W. Deeg *et al.*, J. Chem. Phys. **93**, 3503 (1990).
- [13] F.W. Deeg *et al.*, Phys. Rev. B **44**, 2830 (1991).
- [14] P.G. de Gennes, *The Physics of Liquid Crystals* (Clarendon, Oxford, 1974).
- [15] K.A. Nelson, J. Appl. Phys. **53**, 6060 (1982).
- [16] G. Schwab, F.W. Deeg, and C. Bräuchle, J. Non-Cryst. Solids **172-174**, 348 (1994).
- [17] A. Mauger and D.L. Mills, Phys. Rev. B **27**, 7736 (1983).